Neuroscience 604 (2026) 33–41

Contents lists available at ScienceDirect

Neuroscience

journal homepage: www.elsevier.com/locate/nsc

Quantitative ultrasound radiofrequency analysis for monitoring Parkinson's disease

Baptiste Bizet [a], Michele Trinchi [a], Francesca Nardello [a], Federica Bombieri [a], Andrea Zignoli [b], Paola Zamparo [a,*], Andrea Monte [a]

[a] Department of Neurosciences, Biomedicine and Movement Sciences, University of Verona, Verona, Italy
[b] Department of Industrial Engineering, University of Trento, Trento, Italy

ARTICLE INFO

Keywords:
Parkinson's disease
Quantitative ultrasound
Nakagami distribution
Radiofrequency imaging
Muscle microstructure
Disease monitoring

ABSTRACT

Current clinical assessments of Parkinson's disease rely largely on functional scales, which lack sensitivity to subtle muscle alterations. Therefore, developing objective and quantitative tools to support both diagnosis and disease monitoring is needed. Quantitative ultrasound radiofrequency imaging, particularly through Nakagami analysis, offers a non-invasive means of characterizing tissue scattering properties that may reflect Parkinson's disease – related effects. This study aimed to assess the feasibility of quantitative ultrasound radiofrequency imaging in identifying muscle alterations and disease severity in individuals with Parkinson's disease. Seventeen individuals with Parkinson's disease and 14 healthy controls participated in this study. Patients with Parkinson's disease were divided into early and late stages based on the Hoehn and Yahr scale. Quantitative ultrasound radiofrequency data were collected on each individual's gastrocnemius medialis, tibialis anterior, triceps brachii, and biceps brachii, and analyzed to estimate the Nakagami *m* parameter. The Nakagami *m* parameter was significantly higher in patients with Parkinson's disease compared to healthy controls across all muscles, with the largest differences in the gastrocnemius medialis. The Nakagami *m* parameter in this muscle was strongly associated with disease severity and showed excellent diagnostic performance. No significant asymmetry was observed between the most and least affected limb. These data indicate that quantitative ultrasound radiofrequency Nakagami imaging can detect muscle microstructural alterations associated with Parkinson's disease and is associated with disease severity. This approach shows strong potential as a rapid, low-cost, and quantitative biomarker for the diagnosis and longitudinal monitoring of Parkinson's disease.

Introduction

Parkinson's disease (PD) is the second most prevalent neurodegenerative disorder following Alzheimer's disease. PD is marked by a set of motor symptoms, including muscular rigidity, postural instability, tremors at rest, and slowed movement (Jankovic, 2008). In developed countries, this progressive condition affects approximately 1% of people aged > 60 years (Ascherio and Schwarzschild, 2016). However, due to the ageing of the global population, the number of individuals living with PD is expected to rise substantially in the next decades (Su et al., 2025).

Significant progress has been made in therapeutic strategies for PD, including pharmacological treatments (e.g., Levodopa, Dopamine agonists, MAO-B inhibitors) and surgical therapies (e.g., deep brain stimulation) (Binde et al., 2020; França et al., 2022). These approaches aim to manage PD symptoms and to maintain, as much as possible, a good quality of life as the disease progresses. One of the most important therapeutic aims is to reduce tremor, rigidity, bradykinesia and postural instability. Indeed, patients with PD experience significant functional disability, impaired work economy, and increased risk of falls (Allen et al., 2010).

Compared to healthy individuals, patients with PD present a reduced

List of abbreviations: ANCOVA, Analysis of covariance; AUROC, Area under the receiver operating characteristic curve; CT, Control group; GM, Gastrocnemius medialis; H&Y, Hoehn-Yahr Scale; IPAQ, International Physical Activity Questionnaire; LAL, Less affected limb; MAL, Most affected limb; PD, Parkinson's disease; PD_E, Early Parkinson's disease; PD_L, Late Parkinson's disease; QUR, Quantitative ultrasound radiofrequency; ROC, Receiver operating characteristic; ROI, Region of interest; UPDRS, Unified Parkinson's disease rating scale; η2, Eta-squared.

* Corresponding author at: Department of Neurosciences, Biomedicine and Movement Sciences, University of Verona, Verona 37131, Italy.
E-mail address: paola.zamparo@univr.it (P. Zamparo).

https://doi.org/10.1016/j.neuroscience.2026.04.002
Received 25 December 2025; Accepted 5 April 2026
Available online 7 April 2026

peak torque during maximal voluntary contractions (Magris et al., 2024; Mak et al., 2012). Muscular rigidity, stiffness and a reduced range of motion, manifesting as increased resistance during passive stretching are among the primary motor manifestations of PD (Berardelli et al., 1983). Recent research has shown that mechanical and structural parameters, particularly muscle–tendon unit stiffness and muscle shape changes, are significantly affected by the disease (Monte et al. 2023) and increase as a function of it. This progressive alteration is correlating with the most important clinical scores (e.g., the Hoehn-Yahr Scale and the Unified Parkinson's Disease Rating Scale (UPDRS)). However, evaluating muscle–tendon mechanics is time-consuming, expensive, and requires many hours of post-processing analysis, making it unsuitable for clinical practice. To support clinicians in optimizing patient care, low-cost, precise, and real-time screening tools are needed to identify PD severity and detect its changes over time.

In the last decade, various imaging techniques have been developed to better characterize tissue mechanical properties in patients with PD. Among them, quantitative ultrasound radiofrequency (QUR) techniques have gained attention in outpatient settings as a fast, cost-effective and accessible alternative. Unlike traditional B-mode grayscale ultrasound, which provides qualitative anatomical insights, QUR quantifies tissue properties by analyzing the interactions of ultrasound waves with tissue microstructures. Starting from the raw radiofrequency waves generated by the ultrasound beamformer, it is possible to apply several signal-processing procedures to quantify physical phenomena associated with the propagation of ultrasound through biological tissues. Among various statistical models for ultrasound tissue characterization, the Nakagami distribution has emerged as the most frequently adopted approach because it offers an effective balance between accuracy and computational simplicity (Oelze and Mamou, 2016; Tsui et al., 2016). Nakagami imaging has already demonstrated success in various applications, including breast tumor classifications (Muhtadi et al., 2023; Oelze and Mamou, 2016; Tsui et al., 2008). Recent studies have shown that Nakagami imaging parameters are associated with disease progression and with functional deterioration in Duchenne muscular dystrophy patients, establishing this method as a reliable and quantifiable approach for disease assessment (Chuang et al., 2025; Weng et al., 2017).

In this study, we investigate the potential of QUR modelling techniques for evaluating muscle characteristics in patients with PD. By analyzing ultrasound backscattered statistics of muscle tissue using the Nakagami distribution, we aimed to determine whether this approach can provide a reliable and quantitative tool to effectively reflect disease severity and monitor disease progression. We hypothesized that the Nakagami *m* parameter would be associated with PD severity, and that the QUR technique can effectively distinguish between PD stages based on clinical scores.

Materials and methods

Population

Based on previous studies (Magris et al., 2024; Martignon et al., 2021; Monte et al., 2023), the desired sample size for each group (PD patients and controls) calculated using statistical software (G*Power), ranged from 12 (for mechanical impairment in PD patients) to 15 (for strength deficit in PD patients). To obtain this sample size, we set the alpha level at 0.05 and the statistical power at 0.8.

Seventeen patients with idiopathic PD and 14 healthy controls were recruited for this study; participants were recruited to form two groups with similar characteristics, especially in terms of physical activity, which was assessed using the IPAQ questionnaire (www.ipaq.ki.se).

Inclusion criteria for PD patients were a diagnosis of idiopathic PD, carried out by a neurologist in accordance with the guidelines established by the London Brain Bank criteria. All subjects belonged to a postural instability and gait disorders phenotype (PIDG). Exclusion criteria for all participants included: (i) cognitive impairment or dementia, (ii) inability to walk independently, and (iii) recent muscle injuries or any musculoskeletal disorders other than PD that could interfere with ultrasound assessment. To ensure optimal data quality and minimise movement artefacts such as tremors or rigidity, all assessments were performed during the "on" phase of dopaminergic medication. Disease severity was classified using the modified Hoehn and Yahr scale (stages 1–5), and motor impairment was quantified using the Unified Parkinson's Disease Rating Scale (UPDRS) Part III. Based on their Hoehn-Yahr (H&Y) scores, patients with PD were stratified into two subgroups: Early-PD (PD_E: H&Y $\leq$ 2) and Late-PD (PD_L: H&Y $>$ 2). This specific classification is commonly adopted in research studies to delineate distinct phases of the disease (Goetz et al., 2004), as H&Y Stage 3 is a critical milestone marking the onset of postural instability. Grouping patients with H&Y $\leq$ 2 includes those who maintain functional independence, while H&Y $>$ 2 includes those with an advanced disease stage characterized by a major shift in motor disability and a higher risk of falls. Demographic and clinical data of patients with PD were extracted from hospital medical records. Healthy adults were recruited to match patients with PD in terms of sex, age, and anthropometric characteristics. The demographic characteristics and physical activity levels of all groups are presented in Table 1.

Ethical considerations

This study was conducted in compliance with the Declaration of Helsinki guidelines for human subject research and received approval from the local ethics committee (protocol number 2021-UNVRCLE-0450152). Written informed consent was obtained from all participants prior to study enrolment.

Study design

All participants completed the International Physical Activity Questionnaire (IPAQ) questionnaire and were tested in a single experimental session. Healthy controls underwent ultrasound examination on their dominant side only. Since PD symptoms often begin on one side, patients with PD were tested twice with the ultrasound protocol: the side that first exhibited symptoms were considered the most affected limb (MAL), while the other side was defined as the less affected limb (LAL). Patients with PD were also tested for the UPDRS Part III assessment, during daily living activities.

Data collection

Ultrasound analysis

Muscle imaging was performed using a portable ultrasound system (ArtUs EXT-1H, Telemed UAB, Vilnius, Lithuania) equipped with a 40 mm linear probe placed longitudinally in the most prominent part of

Table 1
Demographic and Anthropometric Characteristics of Study Groups.

	Controls (n = 14; W = 8)	PD_E (n = 7; W = 5)	PD_L (n = 10; W = 5)
Age (year)	69.7 ± 3.7*	68.9 ± 6.9*	77.0 ± 6.2
Body Mass (kg)	70.3 ± 9.6	67.9 ± 10.9	73.4 ± 16.2
Height (cm)	166.2 ± 7.3	163.9 ± 9.4	167.9 ± 11.4
Activity level (MET-minutes/week)	3212 ± 1615	2821 ± 2038	2232 ± 2141
Hoehn and Yahr scale	–	1 [1.5]	3 [1]
UPDRS (Part III)	–	20.3 ± 12.1	67.1 ± 27.6
Duration of the disease (Years)	–	7.1 ± 5.6	5.6 ± 3.9

Note. Values are presented as mean ± standard deviation, except for Hoehn and Yahr data, which are presented as median [interquartile range].
W, Women; PD_E, early Parkinson's disease; PD_L: late Parkinson's disease; UPDRS, Unified Parkinson's Disease Rating Scale.
*Significant difference ($p < 0.05$) with PD_L.

each investigated muscle (L15-7H40-A5 model, 192 elements, 7.5–15 MHz frequency range, 40 MHz sampling frequency, Telemed UAB, Vilnius, Lithuania). The imaging focus and depth were respectively set at 2 and 4 cm. Four muscles were examined two times each in a random order: biceps brachii (long-head), triceps brachii (long-head), tibialis anterior, and gastrocnemius medialis (GM). Participants were seated on an ordinary chair with the hip, knee, ankle, and elbow joints positioned at 90° using a manual goniometer. For upper-limb imaging, the hand was placed on the thigh in a pronated position. Participants were instructed to remain still and as relaxed as possible during image acquisition, which was performed by an experienced investigator. The data which contained the radiofrequency signals were saved as.bin files.

Questionnaires

Physical activity levels were evaluated using the IPAQ, which quantifies intensity and duration of physical activity over the preceding seven days, including walking, moderate-intensity, and vigorous activities (Craig et al., 2003). Patients with PD underwent additional motor performance assessment using the UPDRS Part III to evaluate functional mobility and motor symptoms. UPDRS assessments were conducted by a clinician and the H&Y score was performed and provided by a neurologist in the days preceding the experiments.

Data analysis

QUR technique

The ultrasound radiofrequency data (i.e. the backscattered signals) were re-shaped into 2-D matrices and processed as images with a custom written Python (version 3.11) script. During this phase, the Hilbert transform was applied to obtain the analytical signal for each scan line, from which the envelop was computed as the magnitude. The detected envelop underwent logarithmic compression to generate the B-mode like image, enhancing the dynamic range for visualization purposes. A simple user interface was developed using the Flask web application framework, which allowed an operator to visualize the B-mode image version of the scans, select a quadrilateral region of interest (ROI) and conduct the analysis. The spatial coordinates for each pixel in the B-mode image were then calculated: the x-coordinates correspond to the beam positions, and the y-coordinates are derived from the sampling frequency and speed of sound. For each image, the complete analysis included the calculation of the Nakagami parameter from image-envelop techniques and the shape and location parameters of the Nakagami. ROIs were selected to include only the muscular tissue (see Fig. 1).

A histogram of grayscale intensity was computed for the ROI and normalized to its maximum value. The resulting histogram describes the probability distribution of pixel intensity values for the ROI. The Nakagami distribution models was used to fit the histogram (Cloutier et al., 2021; Ho et al., 2013; Shankar, 2000). This distribution can be described with a shape parameter m and a scaling parameter Ω. The parameters values were estimated using the *scipy* Python, which applies maximum likelihood estimation (Harris-Love et al., 2019).

Weng et al. (2017) explained that the Nakagami m parameter characterizes the scattering conditions within a resolution cell. Specifically, values of $m < 0.5$ correspond to a Nakagami-gamma distribution, indicating a small number of scatterers with gamma-distributed scattering cross-sections. When $0.5 < m < 1$, the distribution is described as pre-Rayleigh, reflecting either a limited number of scatterers or the coexistence of strong and randomly distributed ones. A m value of 1 denotes a Rayleigh distribution, typical of media containing many randomly

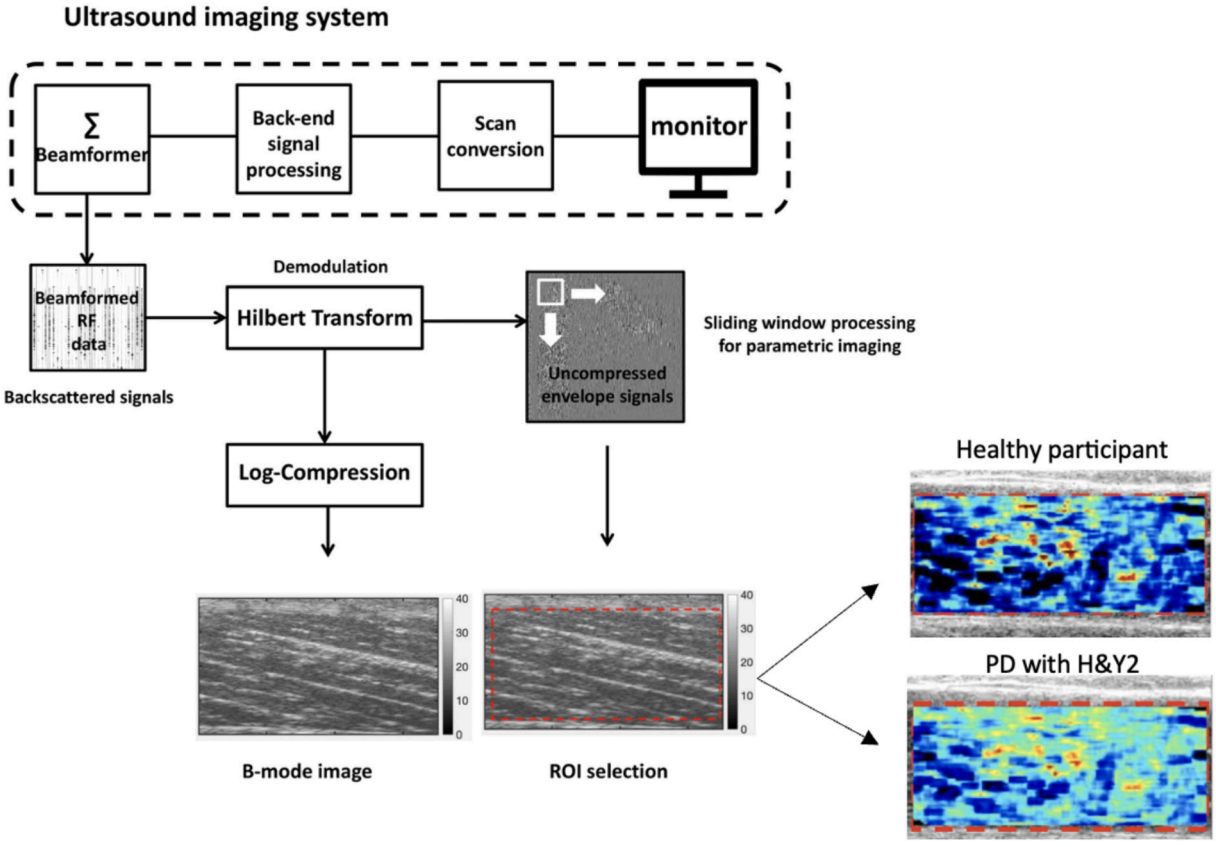

Fig. 1. Schematic representation of the basic steps for RF data analysis. Raw data were used to obtain the envelope image by using the absolute value of the Hilbert Transform. Then, log-compressed envelope was used to obtain Bmode images. The uncompressed envelope image was utilized to identify the region of interest (ROI). The Nakagami parameter was calculated as the mean value of each pixel within the ROI. Two representative Nakagami images for a healthy participant and a PD patient are reported.

distributed scatterers. Finally, when $m > 1$, the distribution becomes post-Rayleigh, therefore suggesting a more organized structure where periodically arranged scatterers coexist with random ones.

Statistical analysis

JASP (version 0.19.3, Amsterdam, The Netherlands) was used for all statistical procedures while R (version 4.3.0) and MATLAB (version R2023b, MathWorks, Natick, Massachusetts, USA) were used for

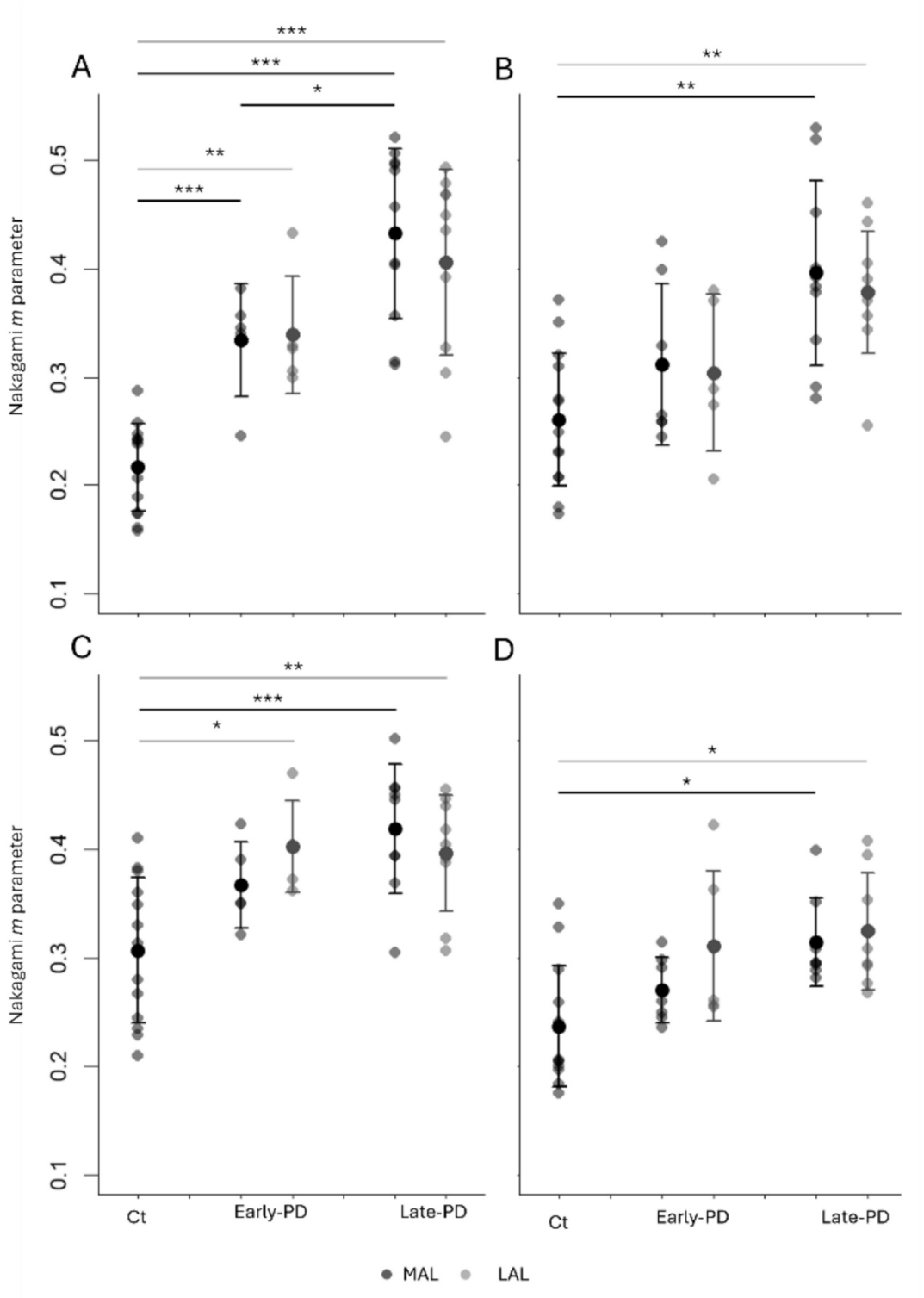

Fig. 2. Nakagami *m* parameter across Parkinson's disease stages in various muscles. Individual data points are shown, overlaid with mean ± SD. Group comparisons were performed using ANCOVA (age as a covariate). CT, control condition; PD_E, early-stage Parkinson's disease; PD_L, late-stage Parkinson's disease; MAL, more affected limb; LAL, less affected limb; A, gastrocnemius medialis; B, tibialis anterior; C, triceps brachii; D, biceps brachii; * $p < 0.05$; ** $p < 0.01$; *** $p < 0.001$ (ANCOVA post-hoc comparisons).

generating the figures. All data are reported as means ± SD. Normality of all variables was assessed using Shapiro-Wilk test, and homogeneity of variances was verified using the Levene's.

A one-way analysis of variances (CT *versus* PD_E *versus* PD_L) revealed a significant difference in age across groups ($F = 8.169$; $p < 0.05$; $\eta^2 = 0.377$). Consequently, age was included as a covariate in all subsequent analyses using analysis of covariances (ANCOVA) to account for its potential confounding effect. Due to the lack of bilateral measurements in the control group (CT), separate analyses were conducted for each side. For the MAL, group (CT *versus* PD_E *versus* PD_L) served as the between-subject factor, with outcome variables as dependent variables and age as covariate. The same approach was applied to the LAL, using the control group for comparison. To assess laterality effects within PD patients, a two-way ANCOVA was performed with side (MAL *versus* LAL) and disease stage (PD_E *versus* PD_L) as between-subject factors, and age as covariate.

All models were checked for assumptions (normality distribution, independence of covariate and treatment, homogeneity of regression slopes, and homoscedasticity). Bonferroni adjustments were performed to account for multiple comparisons between groups. Between-group ANCOVA-derived (adjusted) mean differences and *p* values were presented. The eta-squared (η^2) values were reported as a measure of effect size. Values of 0.01, 0.06, and 0.14 were respectively considered benchmarks for small, medium, and large effects (Richardson, 2011). When significant main or interaction effects were found, Bonferroni-corrected post hoc analyses were conducted, and pairwise mean differences, t values, p values and Cohen's d were reported. The level of statistical significance was set at $p < 0.05$.

Receiver operating characteristic (ROC) curve analysis with 95% confidence intervals (IC) was conducted to calculate the area under the curve (AUROC), and to assess the predictive value of the QUR parameters for diagnosing functional capacity according to the H&Y scale. Two levels were tested: firstly, the capability of the technique to discriminate between healthy individuals and patients (CT *versus* PD_E and PD_L), secondly between controls with early-stage patients and late-stage patients (CT and PD_E *versus* PD_L). Sensitivity, specificity, and accuracy were subsequently derived.

Finally, possible associations between the H&Y scale and QUR imaging were checked using the Kendall's Tau-b correlation as the H&Y scale is ordinal.

Results

No significant differences were observed among groups in body mass, body height and physical activity level (see Table 1). However, PD_L patients were older than healthy controls and PD_E.

Fig. 2 presents the Nakagami *m* parameter among populations and between body sides (for patients with PD only). Nakagami *m* parameter differed significantly between populations in all investigated muscles: patients with PD had higher values of Nakagami *m* parameter when compared to healthy controls (see Fig. 2 and Table 2). No significant differences were seen between MAL and LAL.

In GM, post-hoc analysis revealed significant differences between Nakagami *m* parameter observed in healthy controls and in patients at both stages; importantly, the difference between the two stages was also significant. The analyses conducted on the triceps brachii identified differences between controls and the two PD stages, but no significant differences were seen between PD_L and PD_E. Nakagami *m* parameter analyzed on the tibialis anterior and on the biceps brachii showed significant differences between healthy controls and PD_L, while no differences were appreciated between healthy controls and PD_E nor between PD stages.

The Kendall's Tau-b coefficients computed between the Nakagami *m* parameter and the H&Y score are reported in Table 3. For all investigated muscles, significant positive correlations were reported between Nakagami *m* parameter and the H&Y score. Moreover, significant

Table 2
ANCOVA and post hoc comparisons of Nakagami parameter values between control (CT), early-stage Parkinson's disease (PD_E), and late-stage Parkinson's disease (PD_L) groups.

		Mean ± SD			ANCOVA			CT − PD_E				CT − PD_L				PD_E − PD_L			
Muscle	Side	CT	PD_E	PD_L	F	p	η^2	SE	t	d	p	SE	t	d	p	SE	t	d	p
Gastrocnemius medialis	MAL	0.22 ± 0.04	0.33 ± 0.05	0.44 ± 0.07	36.746	< 0.001***	0.734	0.027	−4.380	−2.167	< 0.001***	0.027	−8.102	−4.003	< 0.001***	0.034	−2.939	−1.836	< 0.05*
	LAL	–	0.34 ± 0.05	0.41 ± 0.09	20.834	< 0.001***	0.619	0.033	−3.858	−2.068	< 0.01**	0.031	−5.656	−2.816	< 0.001***	0.042	−1.101	−0.748	0.844
Tibialis anterior	MAL	0.30 ± 0.10	0.32 ± 0.08	0.40 ± 0.08	6.032	< 0.01**	0.305	0.034	−1.579	−0.736	0.378	0.036	−3.392	−1.667	< 0.01**	0.043	−1.590	−0.931	0.371
	LAL	–	0.30 ± 0.07	0.38 ± 0.06	6.000	< 0.01**	0.316	0.033	−1.551	−0.831	0.401	0.031	−3.281	−1.634	< 0.01**	0.042	−1.181	−0.803	0.746
Triceps brachii	MAL	0.31 ± 0.07	0.37 ± 0.04	0.42 ± 0.06	8.828	< 0.001***	0.421	0.031	−1.621	−0.866	0.356	0.029	−4.759	−2.360	< 0.001***	0.038	−2.298	−1.494	0.093
	LAL	–	0.39 ± 0.05	0.40 ± 0.05	11.539	< 0.001***	0.468	0.031	−3.083	−1.623	< 0.05*	0.030	−3.616	−1.822	< 0.01**	0.036	−0.323	−0.199	1.000
Biceps brachii	MAL	0.24 ± 0.06	0.27 ± 0.03	0.31 ± 0.04	4.753	< 0.05*	0.275	0.022	−1.527	−0.718	0.418	0.023	−3.008	−1.483	< 0.05*	0.027	−1.334	−0.765	0.582
	LAL	–	0.31 ± 0.07	0.33 ± 0.05	5.536	< 0.05*	0.323	0.029	−2.579	−1.284	< 0.05*	0.030	−2.666	−1.358	< 0.05*	0.037	−0.119	−0.074	1.000

Note. CT, control condition; PD_E, early-stage Parkinson's disease; PD_L, late-stage Parkinson's disease; MAL, more affected limb; LAL, less affected limb; SE, standard error; d, Cohen's d effect size; η^2, Eta squared effect size. Significance levels: * $p < 0.05$, ** $p < 0.01$, *** $p < 0.001$. Dashes (–) indicate data not available for CT condition in LAL measurements.
Statistical Analysis: ANCOVA was performed to assess main effect across conditions, followed by pairwise post-hoc comparisons with Bonferroni correction. Effect sizes are reported as Cohen's d for pairwise comparisons and η^2 for ANCOVA main effects.

Table 3
Associations between Nakagami parameter and Hoehn and Yahr scores.

	MAL		LAL	
	Kendall's tau B	p value	Kendall's tau B	p value
Gastrocnemius medialis	0.654	<0.001***	0.587	<0.001***
Tibialis anterior	0.408	<0.01**	0.399	<0.01**
Triceps brachii	0.497	<0.001***	0.430	<0.01**
Biceps brachii	0.405	<0.01**	0.460	<0.001***

Note. MAL, most affected limb; LAL, less affected limb.
Significance levels: * $p < 0.05$, ** $p < 0.01$, *** $p < 0.001$.

positive correlations were observed for both body sides. The highest determination coefficient (Kendall's Tau-b) was observed using the GM Nakagami *m* parameter.

Fig. 3 shows the ROC curves for all investigated muscles and both body sides. ROC curves have been obtained using the Nakagami *m* parameters and the H&Y score. The ROC curves results ranged from good to excellent specificity and sensitivity. In this regard, the models based on the GM yielded the best results with AUROC values of 0.987 (95% IC: [0.943—1.000]) on the MAL and 0.986 (95% IC: [0.938—1.000]) on the LAL (see Fig. 3 for further details related to the other muscles). In both sides, GM and Triceps muscles and in LAL Biceps muscle, AUROC gave better value when testing controls *versus* all PD patients than when testing CT and PD_E *versus* PD_L.

Discussion

This study aimed to evaluate the potential application of a new QUR technique to monitor PD. The main findings were that the Nakagami *m* parameter was able to distinguish healthy individuals from patients with PD and, in some cases, to identify PD severity, providing a new perspective for the clinical evaluation.

An increase in the Nakagami *m* parameter was observed with disease progression which aligns with previous studies in other pathological populations (Chuang et al., 2025; Weng et al., 2017). This increase could reflect a long-term muscle tissue reorganization. The motor-unit remodeling process, including denervation-renervation, leads to an increase in myofiber group size (Kelly et al., 2018) and fiber type shifts (Lavin et al., 2020; Rossi et al., 1996) that may create changes in the scattering micro-structures. For example, Chiang et al. (2019) reported significant differences in intramuscular fat infiltration between healthy older adults and patients with PD. These microstructural changes in muscle composition are likely to influence quantitative ultrasound results, providing a valuable tool for identifying muscle modification related to PD.

Despite the changes observed in Nakagami *m* parameter across different stages of the disease, this parameter alone cannot serve as standalone indicator of disease progression. Previous studies reported reduced muscle strength, power, and rate of force development in individuals with PD (Gamborg et al., 2023), supporting the notion that muscle quality degradation contributes to the functional deterioration characteristic of the condition. Moreover, lower handgrip strength and slower walking speed before the first symptoms have been associated with an increased risk of developing PD as well as with greater disease severity (Hu et al., 2024; Liu et al., 2024). Coupling Nakagami *m* parameter with functional assessments such as handgrip strength, gait speed analysis, and usual clinical scales could provide valuable support to the clinician's evaluation. This combined approach may offer a more comprehensive understanding of disease progression by connecting objective and quantitative indicators of muscle structure to functional and clinical outcomes.

The AUROC values suggest that Nakagami *m* parameter hold promise as complementary markers for distinguishing patients with PD from healthy individuals. Although not yet specific or sensitive enough for clinical diagnosis on their own, these findings open the door for the use of QUR in early detection frameworks when combined with other clinical and biomechanical measures. Moreover, with appropriate caution, these parameters could also help in discriminating disease progression, particularly in the GM, as the AUROC values suggest potential for distinguishing early *versus* later stages of the condition.

No significant differences were found between sides in Nakagami *m* parameter, regardless of disease stage. This suggests that evaluating a single side may be sufficient for both clinical and research purposes. This could reduce the time required for clinicians to perform such analyses in real-life conditions. This is also relevant for simplifying experimental protocols and minimizing patient burden in future studies.

Since PD typically progresses asymmetrically (Uitti et al., 2005), the absence of side differences observed may indicate that this asymmetry is not primarily driven by changes in muscle microstructure. If the muscle microstructure alone may not account for the asymmetrical manifestation of PD, it implies that the early lateralization of symptoms likely originates from neural mechanisms rather than intrinsic muscular alterations.

In our study, the strongest association between Nakagami *m* parameter and PD stage was observed in the GM of the most affected limb (GM-MAL; Kendall's Tau-b = 0.667, $p < 0.001$), revealing the potential relevance of this muscle in reflecting disease-related alterations. This strong association observed in the GM may also be explained by the current clinical evaluation frameworks, which largely rely on mobility-related criteria (Goetz et al., 2004), as the GM plays a central role in gait and balance control (Francis et al., 2013).

Limitations and further considerations

This study involved a small sample size, with seven participants classified as early-stage PD and ten as late-stage PD.

However, a posteriori power analyses revealed that with our total sample size of N = 31 (3 groups, 1 covariate), and considering our observed effect sizes for the Nakagami m parameter (η^2 ranging from 0.275 to 0.734, corresponding to Cohen's f of 0.61 to 1.66), the statistical power (1-β) exceeds 0.83 in the most conservative case and reaches 0.99 for our primary outcome.

Finally, all assessments were performed in patients who had already been diagnosed with PD. To establish a stronger and more direct link between quantitative ultrasound parameters and both the onset and progression of the disease, future large-scale longitudinal studies are needed. Such studies should include healthy individuals without symptoms at baseline and follow them over several years to determine whether the Nakagami m parameter or other QUS metrics can detect early microstructural changes that precede the clinical manifestation of PD and monitor its progression over time. This study provides foundation to implement these simple scanning techniques in an outpatient setting.

This study suggests that the Nakagami *m* parameter derived from quantitative ultrasound radiofrequency data can distinguish healthy individuals from patients with Parkinson's disease and reflects disease severity. Among the investigated muscles, the gastrocnemius medialis showed the strongest association with clinical stage which reveals its potential as a sensitive marker of disease-related changes. Although

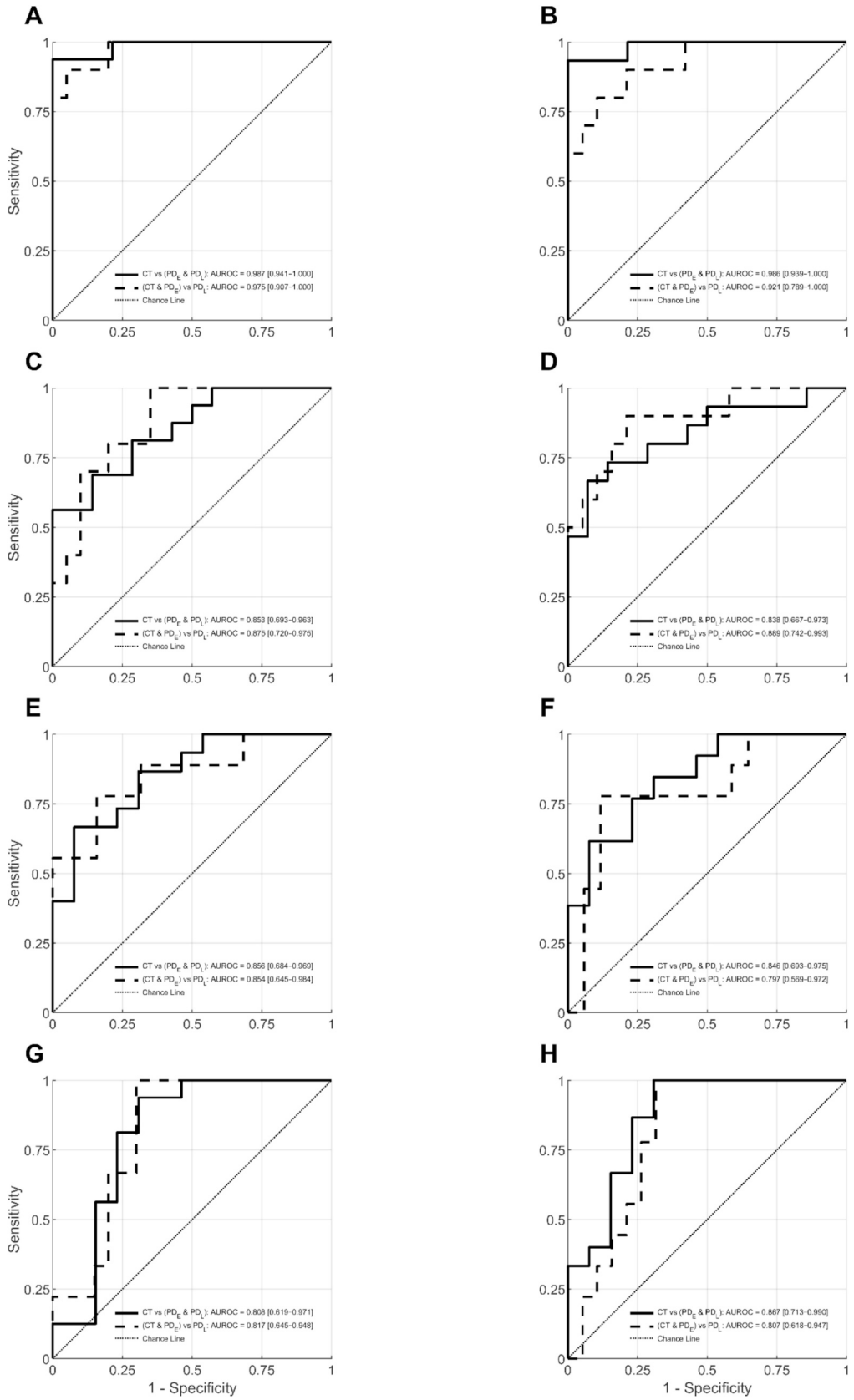

Fig. 3. Receiver Operating Characteristic (ROC) curves for the Nakagami parameter in discriminating between patients with Parkinson's disease and healthy controls. The panels present the True Positive Rate (Sensitivity) plotted against the False Positive Rate (1 − Specificity), with the Area Under the ROC Curve (AUROC) value reported in each graph. The highest discriminatory performance was observed in gastrocnemius medialis for both limbs. Panels are organized by muscle and limb: (A-B) gastrocnemius medialis, (C-D) tibialis anterior, (E-F) triceps brachii, and (G-H) biceps brachii. For each muscle, the left panel represents the most affected limb (MAL) and the right panel the less affected limb (LAL). CT, control condition; PD_E, early-stage Parkinson's disease; PD_L, late-stage Parkinson's disease.

further validation in larger, longitudinal cohorts is required, these findings suggest that quantitative ultrasound radiofrequency techniques could represent a valuable, low-cost, and accessible tool for monitoring muscle alterations and supporting clinical assessment in Parkinson's disease.

CRediT authorship contribution statement

Baptiste Bizet: Writing – review & editing, Writing – original draft, Visualization, Methodology, Investigation, Conceptualization. **Michele Trinchi:** Investigation. **Francesca Nardello:** Writing – review & editing, Resources, Investigation. **Federica Bombieri:** Resources, Investigation. **Andrea Zignoli:** Writing – review & editing, Software. **Paola Zamparo:** Writing – review & editing, Supervision, Funding acquisition. **Andrea Monte:** Writing – review & editing, Writing – original draft, Supervision, Methodology, Funding acquisition, Conceptualization.

Declaration of competing interest

The authors declare that they have no known competing financial interests or personal relationships that could have appeared to influence the work reported in this paper.

Acknowledgment

The authors would like to express their sincere gratitude to all the participants who took part in this study for their time, cooperation, and contribution to the research.

Funding

This study was financially supported by Programma Operativo Nazionale "Ricerca e Innovazione" 2014-2020 (PONRI) [https://www.ponricerca.gov.it/] in the form of a grant ((FSE REACT EU-PON R&I 2014-2020) protocol nr. 405695) received by AM. The first author had a research contract co-financed by the European Union - Programma Operativo Nazionale "Ricerca e Innovazione" 2014-2020 (PONRI), pursuant to article 24, paragraph 3, letter "A", of Law 30 (December 2010, n.240), and subsequent amendments to the Ministerial Decree (10 August 2021 (n. 1062)). The funders had no role in study design, data collection and analysis, decision to publish, or preparation of the manuscript.

References

Allen, N.E., Sherrington, C., Canning, C.G., Fung, V.S.C., 2010. Reduced muscle power is associated with slower walking velocity and falls in people with Parkinson's disease. Parkinsonism Relat. Disord. 16 (4), 261–264. https://doi.org/10.1016/j.parkreldis.2009.12.011.

Ascherio, A., Schwarzschild, M.A., 2016. The epidemiology of Parkinson's disease: risk factors and prevention. Lancet Neurol. 15 (12), 1257–1272. https://doi.org/10.1016/S1474-4422(16)30230-7.

Berardelli, A., Sabra, A.F., Hallett, M., 1983. Physiological mechanisms of rigidity in Parkinson's disease. J. Neurol. Neurosurg. Psychiatry 46 (1), 45–53. https://doi.org/10.1136/jnnp.46.1.45.

Binde, C.D., Tvete, I.F., Gåsemyr, J.I., Natvig, B., Klemp, M., 2020. Comparative effectiveness of dopamine agonists and monoamine oxidase type-B inhibitors for Parkinson's disease: a multiple treatment comparison meta-analysis. Eur. J. Clin. Pharmacol. 76 (12), 1731–1743. https://doi.org/10.1007/s00228-020-02961-6.

Chiang, P.-L., Chen, Y.-S., Lin, A.-W.-C., 2019. Altered body composition of psoas and thigh muscles in relation to frailty and severity of Parkinson's disease. Int. J. Environ. Res. Public Health 16 (19), 3667. https://doi.org/10.3390/ijerph16193667.

Chuang, Y.-W., Lin, C.-W., Weng, W.-C., Tsui, P.-H., 2025. Ultrasound scatteromics: a multimodal QUS-based solution for detecting ambulatory function deterioration in Duchenne muscular dystrophy. Ultrasonics 154, 107679. https://doi.org/10.1016/j.ultras.2025.107679.

Cloutier, G., Destrempes, F., Yu, F., Tang, A., 2021. Quantitative ultrasound imaging of soft biological tissues: a primer for radiologists and medical physicists. Insights Imaging 12 (1), 127. https://doi.org/10.1186/s13244-021-01071-w.

Craig, C.L., Marshall, A.L., Sjöström, M., Bauman, A.E., Booth, M.L., Ainsworth, B.E., Pratt, M., Ekelund, U., Yngve, A., Sallis, J.F., Oja, P., 2003. International physical activity questionnaire: 12-country reliability and validity. Med. Sci. Sports Exerc. 35 (8), 1381–1395. https://doi.org/10.1249/01.MSS.0000078924.61453.FB.

França, C., Carra, R.B., Diniz, J.M., Munhoz, R.P., Cury, R.G., 2022. Deep brain stimulation in Parkinson's disease: state of the art and future perspectives. Arq. Neuropsiquiatr. 80 (5 Suppl 1), 105–115. https://doi.org/10.1590/0004-282X-ANP-2022-S133.

Francis, C.A., Lenz, A.L., Lenhart, R.L., Thelen, D.G., 2013. The modulation of forward propulsion, vertical support, and center of pressure by the plantarflexors during human walking. Gait Posture 38 (4), 993–997. https://doi.org/10.1016/j.gaitpost.2013.05.009.

Gamborg, M., Hvid, L.G., Thrue, C., Johansson, S., Franzén, E., Dalgas, U., Langeskov-Christensen, M., 2023. Muscle strength and power in people with Parkinson disease: a systematic review and meta-analysis. J. Neurol. Phys. Ther. 47 (1), 3. https://doi.org/10.1097/NPT.0000000000000421.

Goetz, C.G., Poewe, W., Rascol, O., Sampaio, C., Stebbins, G.T., Counsell, C., Giladi, N., Holloway, R.G., Moore, C.G., Wenning, G.K., Yahr, M.D., Seidl, L., 2004. Movement disorder society task force report on the Hoehn and Yahr staging scale: status and recommendations. Mov. Disord. 19 (9), 1020–1028. https://doi.org/10.1002/mds.20213.

Harris-Love, M.O., Gonzales, T.I., Wei, Q., Ismail, C., Zabal, J., Woletz, P., DiPietro, L., Blackman, M.R., 2019. Association between muscle strength and modeling estimates of muscle tissue heterogeneity in young and old adults. J. Ultrasound Med. 38 (7), 1757–1768. https://doi.org/10.1002/jum.14864.

Ho, M.-C., Lee, Y.-H., Jeng, Y.-M., Chen, C.-N., Chang, K.-J., Tsui, P.-H., 2013. Relationship between ultrasound backscattered statistics and the concentration of fatty droplets in livers: an animal study. PLoS One 8 (5), e63543. https://doi.org/10.1371/journal.pone.0063543.

Hu, W., Zhao, C.-H., Huang, Y.-Q., Liu, B.-P., Jia, C.-X., 2024. Grip strength, genetic predisposition, and incident Parkinson's disease: a prospective cohort study in the UK biobank. NPJ Parkinson's Dis. 10 (1), 191. https://doi.org/10.1038/s41531-024-00810-2.

Jankovic, J., 2008. Parkinson's disease: clinical features and diagnosis. J. Neurol. Neurosurg. Psychiatry 79 (4), 368–376. https://doi.org/10.1136/jnnp.2007.131045.

Kelly, N.A., Hammond, K.G., Bickel, C.S., Windham, S.T., Tuggle, S.C., Bamman, M.M., 2018. Effects of aging and Parkinson's disease on motor unit remodeling: influence of resistance exercise training. J. Appl. Physiol. 124 (4), 888–898. https://doi.org/10.1152/japplphysiol.00563.2017.

Lavin, K.M., Sealfon, S.C., McDonald, M.-L.-N., Roberts, B.M., Wilk, K., Nair, V.D., Ge, Y., Lakshman Kumar, P., Windham, S.T., Bamman, M.M., 2020. Skeletal muscle transcriptional networks linked to type I myofiber grouping in Parkinson's disease. J. Appl. Physiol. 128 (2), 229–240. https://doi.org/10.1152/japplphysiol.00702.2019.

Liu, M., He, P., Ye, Z., Zhang, Y., Zhou, C., Yang, S., Zhang, Y., Qin, X., 2024. Association of handgrip strength and walking pace with incident Parkinson's disease. J. Cachexia. Sarcopenia Muscle 15 (1), 198–207. https://doi.org/10.1002/jcsm.13366.

Magris, R., Nardello, F., Bombieri, F., Monte, A., Zamparo, P., 2024. Characterization of the vastus lateralis torque-length, and knee extensors torque-velocity and power-velocity relationships in people with Parkinson's disease. Front. Sports Active Living 6, 1380864. https://doi.org/10.3389/fspor.2024.1380864.

Mak, M.K.Y., Pang, M.Y.C., Mok, V., 2012. Gait difficulty, postural instability, and muscle weakness are associated with fear of falling in people with Parkinson's disease. Parkinson's Disease 2012, 901721. https://doi.org/10.1155/2012/901721.

Martignon, C., Ruzzante, F., Giuriato, G., Laginestra, F.G., Pedrinolla, A., Di Vico, I.A., Saggin, P., Stefanelli, D., Tinazzi, M., Schena, F., Venturelli, M., 2021. The key role of physical activity against the neuromuscular deterioration in patients with Parkinson's disease. Acta Physiol. 231 (4), e13630. https://doi.org/10.1111/apha.13630.

Monte, A., Magris, R., Nardello, F., Bombieri, F., Zamparo, P., 2023. Muscle shape changes in Parkinson's disease impair function during rapid contractions. Acta Physiol (Oxf.) 238 (1). https://doi.org/10.1111/apha.13957.

Muhtadi, S., Razzaque, R.R., Chowdhury, A., Garra, B.S., Kaisar Alam, S., 2023. Texture quantified from ultrasound Nakagami parametric images is diagnostically relevant for breast tumor characterization. J. Med. Imaging 10 (Suppl 2), S22410. https://doi.org/10.1117/1.JMI.10.S2.S22410.

Oelze, M.L., Mamou, J., 2016. Review of quantitative ultrasound: envelope statistics and backscatter coefficient imaging and contributions to diagnostic ultrasound. IEEE Trans. Ultrason. Ferroelectr. Freq. Control 63 (2), 336–351. https://doi.org/10.1109/TUFFC.2015.2513958.

Richardson, J.T.E., 2011. Eta squared and partial eta squared as measures of effect size in educational research. Educ. Res. Rev. 6 (2), 135–147. https://doi.org/10.1016/j.edurev.2010.12.001.

Rossi, B., Siciliano, G., Carboncini, M.C., Manca, M.L., Massetani, R., Viacava, P., Muratorio, A., 1996. Muscle modifications in Parkinson's disease: myoelectric manifestations. Electroencephalogr. Clin. Neurophysiol. 101 (3), 211–218. https://doi.org/10.1016/0924-980x(96)94672-x.

Shankar, M., 2000. A general statistical model for ultrasonic backscattering from tissues. IEEE Trans. Ultrason. Ferroelectr. Freq. Control 47 (3), 727–736. https://doi.org/10.1109/58.842062.

Su, D., Cui, Y., He, C., Yin, P., Bai, R., Zhu, J., Lam, J.S.T., Zhang, J., Yan, R., Zheng, X., Wu, J., Zhao, D., Wang, A., Zhou, M., Feng, T., 2025. Projections for prevalence of Parkinson's disease and its driving factors in 195 countries and territories to 2050: modelling study of Global Burden of Disease Study 2021. BMJ 388, e080952. https://doi.org/10.1136/bmj-2024-080952.

Tsui, P.-H., Ho, M.-C., Tai, D.-I., Lin, Y.-H., Wang, C.-Y., Ma, H.-Y., 2016. Acoustic structure quantification by using ultrasound Nakagami imaging for assessing liver fibrosis. Sci. Rep. 6 (1), 33075. https://doi.org/10.1038/srep33075.

Tsui, P.-H., Yeh, C.-K., Chang, C.-C., Liao, Y.-Y., 2008. Classification of breast masses by ultrasonic Nakagami imaging: a feasibility study. Phys. Med. Biol. 53 (21), 6027–6044. https://doi.org/10.1088/0031-9155/53/21/009.

Uitti, R.J., Baba, Y., Wszolek, Z.K., Putzke, D.J., 2005. Defining the Parkinson's disease phenotype: initial symptoms and baseline characteristics in a clinical cohort. Parkinsonism Relat. Disord. 11 (3), 139–145. https://doi.org/10.1016/j.parkreldis.2004.10.007.

Weng, W.-C., Tsui, P.-H., Lin, C.-W., Lu, C.-H., Lin, C.-Y., Shieh, J.-Y., Lu, F.L., Ee, T.-W., Wu, K.-W., Lee, W.-T., 2017. Evaluation of muscular changes by ultrasound Nakagami imaging in Duchenne muscular dystrophy. Sci. Rep. 7 (1), 1. https://doi.org/10.1038/s41598-017-04131-8.